# REPORT DOCUMENTATION PAGE

Form Approved OMB No. 0704-0188

| 1. AGENCY USE ONLY (Leave blank) | 2. REPORT DATE<br><br>5 January 2001 | 3. REPORT TYPE AND DATES COVERED<br><br>Final Report |
|---|---|---|

**4. TITLE AND SUBTITLE**

Bridges of Periodic Solutions and Tori in Semiconductor Lasers Subject to Delay

**5. FUNDING NUMBERS**

F61775-00-WE

**6. AUTHOR(S)**

Dr. Thomas Erneux

**7. PERFORMING ORGANIZATION NAME(S) AND ADDRESS(ES)**

Universite Libre de Bruxelles
Campus Plaine, CP 231
Bld du Triomphe
Brussels B-1050
Belgium

**8. PERFORMING ORGANIZATION REPORT NUMBER**

N/A

**9. SPONSORING/MONITORING AGENCY NAME(S) AND ADDRESS(ES)**

EOARD
PSC 802 BOX 14
FPO 09499-0200

**10. SPONSORING/MONITORING AGENCY REPORT NUMBER**

SPC 00-4021

**11. SUPPLEMENTARY NOTES**

**12a. DISTRIBUTION/AVAILABILITY STATEMENT**

Approved for public release; distribution is unlimited.

**12b. DISTRIBUTION CODE**

A

**13. ABSTRACT (Maximum 200 words)**

This report results from a contract tasking Universite Libre de Bruxelles as follows: The contractor will investigate the use of Lang and Kobayashi equations for modeling a laser subject to optical feedback. The final report is a draft paper for publication, entitled: "Bridges of periodic solutions and tori in semiconductor lasers subject to delay" by D. Pieroux, T. Erneux, B. Haegeman, T. Luzyanina, K. Engelborghs, and D. Roose.

| 14. SUBJECT TERMS | | | | 15. NUMBER OF PAGES |
|---|---|---|---|---|
| EOARD, semiconductor lasers, Fibre lasers | | | | 14 |
| | | | | **16. PRICE CODE**<br>N/A |

| 17. SECURITY CLASSIFICATION OF REPORT | 18. SECURITY CLASSIFICATION OF THIS PAGE | 19. SECURITY CLASSIFICATION OF ABSTRACT | 20. LIMITATION OF ABSTRACT |
|---|---|---|---|
| UNCLASSIFIED | UNCLASSIFIED | UNCLASSIFIED | UL |

# Bridges of periodic solutions and tori in semiconductor lasers subject to delay

D. Pieroux and T. Erneux

*Université Libre de Bruxelles, Optique Nonlinéaire Théorique,*

*Campus Plaine, C.P. 231, 1050 Bruxelles, Belgium*

B. Haegeman, T. Luzyanina, K. Engelborghs and D. Roose

*Department of Computer Science, K.U. Leuven, Celestijnenenlaan 200A,*

*3001 Heverlee, Belgium*

(January 5, 2001)

## Abstract

For semiconductor lasers subject to a delayed optical feedback, branches of steady states sequentially appear as the feedback rate is increased. But branches of time-periodic solutions are connecting pairs of steady states and provide bridges between stable and unstable modes. All bridges experience a change of stability through a torus bifurcation point. Close to the bifurcation point, the torus remains localized near a specific fixed point in phase space. As the feedback rate increases, the torus envelope suddenly unfolds and its trajectory visits two or more unstable fixed points, anticipating the rich dynamics observed at larger feedback rates.

42.60.Mi, 42.55.-f, 42.55.Px

1

Nonlinear problems with a delayed feedback appear in many areas of science and engineering. They are modeling problems in chemistry (diffusion through a membrane, illuminated thermochemical reaction [1]), in biology (blood cell production [2,3], neural control [4], respiratory physiology [5]), in the medical sciences (drug delivery [6]), in mechanics (ship rolling [7]), as well as many other physical problems [8]. In nonlinear optics, a delayed feedback often plays an active role in the device. It may be used to stabilize a laser [9] or to deliberately produce a chaotic output [10]. It may also considerably diminish the performances of semiconductor lasers. These lasers appear in many of our applications (laser printer, CD player, code bar reading at the supermarket) and are highly sensible to delayed optical feedback. A weak optical feedback from external reflectors like the front facet of an optical fiber, a mirror, or an optical disk is enough to destabilize the normal output of the laser.

For lasers controlled by feedback or subject to an unwanted feedback as well as other physical or biological systems modeled by delay-differential equations, the delay may have a stabilizing or a destabilizing effect. In many cases, however, we observe cascading instabilities which lead to complex dynamical regimes. Combined analytical and numerical studies of delay-differential equations (DDE) remain rare and it is not surprising that a lot of our current efforts on DDE concentrate on specific problems in nonlinear optics. In particular, a semiconductor laser subject to a delayed optical feedback is a key problem for all semiconductor laser devices. Most of our understanding of its behavior comes from numerical studies [11]. One interesting dynamical regime, called Low Frequency Fluctuation or LFF, has attracted a lot of attention. If a semiconductor laser operates close to its threshold, the laser power exhibits irregular oscillations with a short and a long time scales. The long time scale is about 100 ns and is characterized by sudden intensity drop-outs. The short time scale is of the order of 1 ps and is much harder to identify [12]. Recent experimental investigations have considerably contributed to our understanding of LFF: a stable steady state mode of operation called the maximum gain mode always exists as an alternate to LFF [13] and LFF appears gradually as the number of modes increase [14]. Theoretically,

new ideas have also appeared. We may benefit from the fact that LFF appears with a low number of modes and investigate the bifurcation diagram analytically [15]. We may simulate the laser equations for a large range of values of the physical parameters and find conditions for which LFF is almost time-periodic (locked states [16]). Last, we may look for simplified forms of the laser equations which produce outputs close to LFF [17,18].

As the feedback rate is progressively increased from zero, branches of steady state intensities appear and are called external cavity modes. Each branch exhibits one of more Hopf bifurcations points which are followed by more complex bifurcations. Direct time integration of the laser equations are limited to the stable solutions. Popular continuation methods such as AUTO [19] are capable to follow stable and unstable time-periodic solutions but are not available for delay differential equations. In this letter, we use a numerical continuation method specially developed for DDE [20] and find a simple bifurcation scenario as the feedback rate increases. Specifically, we find closed branches of periodic solutions connecting pairs of isolated steady states and torus bifurcation points which mark the beginning of richer time-dependent regimes.

A single mode semiconductor laser subject to weak and moderate optical feedback is modeled by the Lang and Kobayashi equations [21]. In dimensionless form, these equations consist of the following two equations for the complex electrical field $Y$ and the excess carrier number $Z$ [17]

$$\frac{dY}{dt} = (1 + i\alpha)YZ + \kappa \exp(-i\omega_0\tau)Y(t - \tau),\tag{1}$$

$$T\frac{dZ}{dt} = P - Z - (1 + 2Z)|Y|^2\tag{2}$$

Time $t$ is measured in units of the photon lifetime $\tau_p$ ($t \equiv t'/\tau_p$). The external round-trip time is normalized as $\tau \equiv 2L/c\tau_p$ where $L$ is the distance laser-mirror and $c$ is the speed of light. $\omega_0 \equiv \omega\tau_p$ is the dimensionless angular frequency of the solitary laser $\omega$, and $\kappa \equiv \gamma\tau_p$ is the normalized feedback rate. $\alpha$ is the linewidth enhancement factor and $T \equiv \tau_n/\tau_p$ is the ratio of the carrier $\tau_s$ to photon lifetime $\tau_p$. $P$ denotes the pumping rate above threshold. Typical values of the parameters are given by [14]

$$T = \tau = 10^3, \ P = 10^{-3}, \ \alpha = 4 \text{ and } \omega_0\tau = -1. \tag{3}$$

We may reduce the number of parameters by introducing the new variables $s$, $E$, and $N$ defined by $s \equiv t/\tau$, $E \equiv \tau^{1/2}Y$ and $N \equiv \tau Z$. In terms of these new variables, Eqs. (1) and (2) become

$$\frac{dE}{ds} = (1 + i\alpha)NE + \eta \exp(-i\omega_0\tau)E(s-1), \tag{4}$$

$$q\frac{dN}{ds} = p - N - (1 + 2\tau^{-1}N)|E|^2 \tag{5}$$

where the parameters $\eta, p$ and $q$ are defined by $\eta \equiv \tau\kappa$, $p \equiv \tau P$ and $q \equiv T\tau^{-1}$. The advantages of the rescaled equations (4) and (5) are twofold. First, using the values of the parameters listed in (3), we find $p = q = 1$. Consequently, the stiffness of the original equations (1) and (2) (large $T$ and $\tau$) has been removed meaning that the new equations (4) and (5) are easier to solve numerically. Second, we may neglect the $\tau^{-1}$ small term in Eq. (5) and reduce the number of fixed parameters.

A basic solution of Eqs. (4) and (5), called a external cavity mode or ECM solution corresponds to a single frequency solution of the form

$$E = A \exp\left(i(\Delta - \omega_0\tau)s\right) \tag{6}$$

and $N = B$ where $A$, $\Delta$ and $B$ are constants. The intensity $|E|^2$ of any ECM mode solution is thus constant and equals $|A|^2$. Substituting (6) into Eqs. (4) and (5) leads to conditions for $A$, $B$ and $\Delta$ which can be analyzed. Specifically, the ECM frequency $\Delta$ satisfies the transcendental equation

$$\Delta - \omega_0\tau = -\eta\left(\alpha\cos(\Delta) + \sin(\Delta)\right) \tag{7}$$

and $A$, $B$ are related to $\Delta$ by $A^2 = \frac{p + \eta\cos(\Delta)}{1 - 2\eta\tau^{-1}\cos(\Delta)} \geq 0$ and $B = -\eta\cos(\Delta)$. By analyzing Eq. (7) in the implicit form $\eta = \eta(\Delta)$, we note that the number of ECM solutions increases with $\eta$. Except for the first ECM solution which appears at $\eta = 0$ or ECM solutions that bifurcate from $A = 0$, all ECM solutions appear by pair and emerge from limit points. One branch

4

of solutions is always unstable (called anti-mode) and the other branch of solutions is stable (called mode) but may experience a change of stability through a Hopf bifurcation. Hopf bifurcation points appear on all (stable or unstable) branches but cannot be determined analytically [22].

In general, bifurcation diagrams are obtained by numerical integration of the laser equations changing gradually the feedback rate [14]. The simulations are limited to the stable regimes and require several runs with different initial conditions in order to detect isolated and/or coexisting solutions. Computations can be costly and have motivated alternative techniques such as the development of numerical continuation methods appropriate for delay-differential equations [20]. A continuation method detects Hopf bifurcation points in parameter space, follow stable or unstable branches of time-periodic solutions, and determine their stability changes. Figure 1 shows the bifurcation diagram of the steady and time-periodic solutions for the values of the parameters listed in (3). Branches of periodic solutions are connecting pairs of mode - antimode solutions. These bridges start and terminate at distinct Hopf bifurcation points (shown by circles in Figure 1). They also overlap points where a mode and an antimode admit the same intensity. A recent asymptotic analysis of Eqs. (1) and (2) valid in the limit of large values of $T$ shows that mixed ECM solutions of the form

$$E \simeq A_1 \exp\left(i(\Delta_1 - \omega_0\tau)s\right) + A_2 \exp\left(i(\Delta_2 - \omega_0\tau)s\right) \tag{8}$$

exist in the vicinity of these points [15]. $\Delta_1$ and $\Delta_2$ are two single ECM frequencies satisfying Eq. (7) evaluated at the equal intensity point. By contrast to the single ECM solution (6), the mixed ECM solution (8) admits a time-periodic intensity $|E|^2$ with a frequency equal to $|\Delta_1 - \Delta_2|$. The amplitudes $A_1$ and $A_2$ are functions of $\eta$ which can be determined by a higher order analysis [15]. By investigating the behavior of the extrema of $|E|$ as a function of $\eta$, we note that the mixed ECM solution (8) corresponds to a closed branch of periodic solutions which overlaps the point where the single modes exhibit the same intensity. Although, the approximation (8) is mathematically valid for $T$ large (equivalently, $q$ large)

5

[15], we have compared analytical and numerical solutions for the first mode - antimode bridge (see Figure 2). The good agreement between the numerical and analytical branches even for $q = 1$ suggests that the mixed ECM solution (8) is a natural approximation of the time-periodic solutions connecting pairs of single ECMs. The interaction between a mode and an antimode also generates a secondary torus bifurcation point (square in Figure 1). This bifurcation is important for the high intensity branches because it marks their change of stability and their transition to more complex regimes.

It is worthwhile to investigate the behavior of the tori as they emerge from their bifurcation points. To this end, we use a standard integration technique and solve numerically Eqs. (4) and (5). We concentrate on the high intensity branches. As the feedback rate surpasses the torus bifurcation point, the oscillations are quasiperiodic and the envelope of the tori remains localized in the vicinity of the original ECM point (see Figure 3a). The oscillations are typically quasiperiodic i.e., a low frequency modulation of rapid oscillations (see Figure 3c). The period of the rapid oscillations is $P \simeq 1.16$ which is close to the analytical estimate $P = 2\pi / |\Delta_2 - \Delta_1| \simeq 1.14$ (here, $\Delta_1 \simeq -17.5$ and $\Delta_2 \simeq -12$ are the frequencies of the two interacting ECMs). Our bifurcation scenario substantiates earlier investigations on high frequency regimes possibly linked to a mode - antimode interaction [23,24]. The period of the slow envelope is about $P \simeq 6.25$ and manifests the effect of the laser relaxation oscillations corrected by the feedback [25]. Above a critical feedback rate, we note a sudden jump to a quite different regime. Specifically, the torus envelope unfolds into a trajectory that is now orbiting near two or more ECM points (see Figure 3b). The time evolution shown in Figure 3d indicates that several unstable single mode or unstable periodic orbits are visited. The common feature between these modes and orbits is that they admit a similar value of $N$ (see Figure 3b). A detailed numerical analysis of the solutions near the transition point between bounded and unbounded tori indicates a slight domain of hysteresis.

The multi-frequency regime appearing as the bounded torus unfolds in the phase plane anticipates the rich dynamics of LFF observed at larger feedback rates. The bifurcation scenario (periodic isola, torus bifurcation, and torus unfolding) repeats itself for each high

6

intensity branch of periodic solutions introducing more periodic orbits and allowing the progressive development of a mature LFF observed at larger values of the feedback rate.

# REFERENCES

[1] I.R. Epstein and J.A. Pojman, "An Introduction to Nonlinear Chemical Dynamics", Oxford University Press, New York 1998.

[2] M. C. Mackey and L. Glass, Science **197**, 287 (1977); L. Glass and M.C. Mackey, Ann. NY. Acad. Sci **316**, 214 (1979).

[3] J.D. Murray, "Mathematical Biology", Biomathematics Texts **19**, Springer-Verlag, Berlin (1980).

[4] A. Longtin and J.G. Milton, Math. Biosci. **90**, 183 (1988); Bull. Math. Biol. **51**, 605 (1989); A. Longtin, J.G. Milton and M.C. Mackey, Phys. Rev. A **41**, 6992 (1990).

[5] A.C. Fowler, "Mathematical Models in the Applied Sciences", Camb. Texts in Applied Mathematics, Camb. Univ. Press, 1997.

[6] J.G. Milton, S.A. Campbell and J. Bélair, J. Biol. Systems **3**, 711 (1995).

[7] N. Minorsky, "Nonlinear Oscillations", D. Van Nostrand Co., Inc, Princeton, 1962.

[8] R.D. Driver, "Ordinary and Delay Differential Equations", Applied Mathematical Sciences 20, Springer-Verlag, Berlin, 1977.

[9] D.J. Gauthier, D. W. Sukow, H.M. Concannon, and J.E.S. Socolar, Phys. Rev. E **50**, 2343 (1994); J.E.S. Socolar, D.W. Sukow and D.J. Gauthier, Phys. Rev. E **50**, 3245 (1994); S. Bielawski, D. Derozier and P. Glorieux, Phys. Rev. E **49**, R971 (1994).

[10] J.-P. Goedgebuer, L. Larger and H. Porte, Phys. Rev. E **57** (1998), 2795; L. Larger, J.-P. Goedgebuer and J.-M. Merolla, IEEE J. Quant. Electr. **34**, 594 (1998).

[11] G.H.M. van Tartwijk, A.M. Levine, D. Lenstra, IEEE J. of Selec. Topics in Quant. Electronics **1**, 466 (1995); J. Mork, B. Tromborg, J. Mark, IEEE J. of Quant. Electronics **28**, 93 (1992); T. Sano Phys. Rev. A **50**, 2719 (1994); C. Masoller and N.B. Abraham, Phys. Rev. A **57**, 1313 (1998); R.L. Davidchack, Y.-C. Lai, A. Gavrielides and V.

Kovanis, Physica D **145**, 130 (2000).

[12] I. Fischer, G.H.M. van Tartwijk, A.M. Levine, W. Elsässer, E. Göbel and D. Lenstra, Phys. Rev. Lett. **76**, 220 (1996).

[13] T. Heil, I. Fischer and W. Elsässer, Phys. Rev. A **58**, R2672 (1998).

[14] A. Hohl and A. Gavrielides, Phys. Rev. Letters **82**, 1148 (1999).

[15] T. Erneux, F. Rogister, A. Gavrielides and V. Kovanis, Opt. Comm. **183**, 467 (2000).

[16] A. Gavrielides, T.C. Newell, V. Kovanis, R.G. Harrison, N. Swanston, D. Yu and W. Lu, Phys. Rev. A **60**, 1577 (1999).

[17] P.M. Alsing, V. Kovanis, A. Gavrielides and T. Erneux, Phys. Rev. A **53**, 4429 (1996).

[18] G. Huet, P.A. Porta, S.P. Hegarty, J.G. McInerney and F. Holland, Opt. Comm. **180**, 339 (2000).

[19] E. Doedel, T. Fairgrieve, B. Sandstede, A. Champneys, Yu. Kuznetsov, and X. Wang, "AUTO 97: Continuation and bifurcation software for ordinary differential equations" http://indy.cs.concordia.ca/auto/main.html.

[20] K. Engelborghs, T. Luzyanina, K. in't Hout and D. Roose, SIAM J.of Sci. Comp. **22**, 1593 (2000); K. Engelborghs, T. Luzyanina, D. Roose, to appear in J. Comp. Appl. Math. **6** (2000); K. Engelborghs."DDE-BIFTOOL: a Matlab package for bifurcation analysis of delay differential equations", http://www.cs.kuleuven.ac.be/~koen/delay/ddebiftool.shtml.

[21] R. Lang and K. Kobayashi. IEEE J. Quant. Electr. QE-16, 347 (1980).

[22] T. Erneux, in Physics and Simulations of Optoelectronic Devices VIII, R. Binder, P. Blood, M. Osinski, Eds., Proc. SPIE **3944**, 588 (2000).

[23] A.A. Tager and B.B. Elenkrig, IEEE J. of Quant. Electron. **29**, 2886 (1993).

[24] A. A. Tager and K. Petermann, IEEE J. of Quant. Electron. **30**, 1553 (1994).

[25] G. Lythe, T. Erneux, A. Gavrielides and V. Kovanis, Phys. Rev. A **55**, 4443 (1997).

**Figure Captions**

Figure 1. Bifurcation diagram of the steady and time-periodic solutions. Full and dashed lines correspond to stable and unstable solutions, respectively. Circles, triangles and squares denote Hopf, period doubling, and torus bifurcation points, respectively. Closed branches of periodic solutions are connecting a mode and an anti-mode. The first branch of periodic solutions admit a closed branch of period two solutions (not shown). A torus bifurcation point immediately follows the second period doubling bifurcation point.

Figure 2. First branch of periodic solutions. Both the maxima and the minima of the oscillations are shown. The numerical branch (full line) is compared to the asymptotic approximation (dashed line). It is given by (8) where $\Delta_1$ and $\Delta_2$ are the single mode ECM frequencies evaluated at the equal intensity point (indicated in the figure by an arrow).
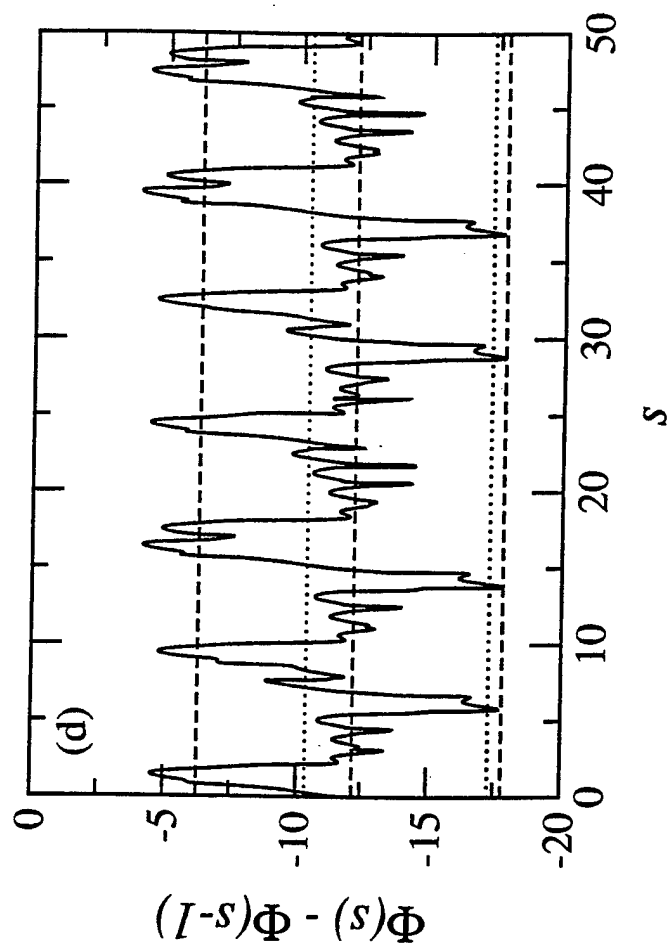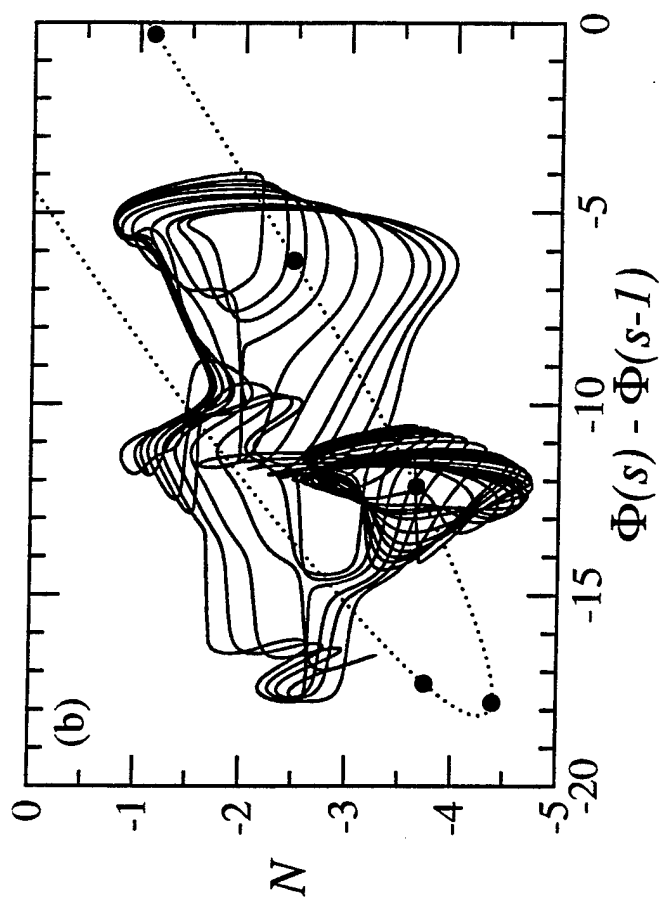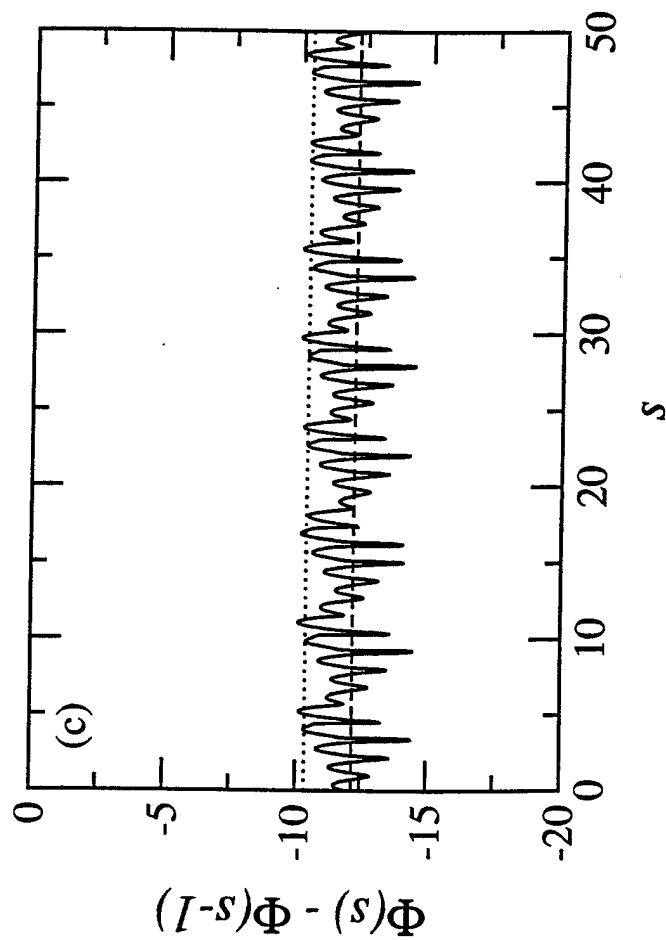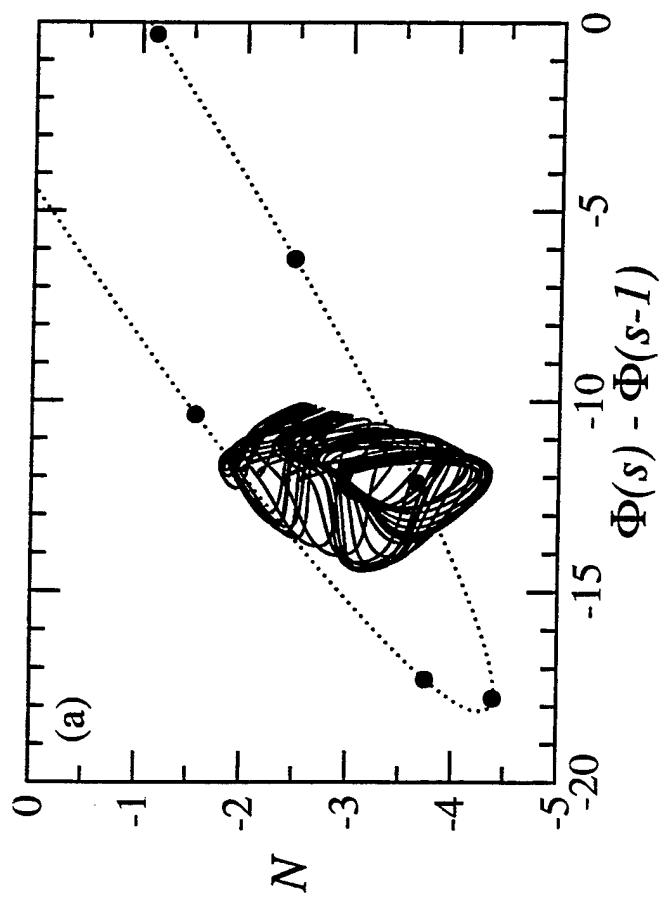
Figure 3. Tori. At a critical feedback rate, a torus oscillating near an unstable periodic orbit suddenly unfolds into a more complex regime. This new regime dominates at higher values of $\eta$ but coexists with the previous torus for a very small domain of $\eta$. The solutions are represented in the phase plane $N$ vs $\Phi(s-1) - \Phi(s)$. We also show $\Phi(s-1) - \Phi(s)$ as a function of time $s$. Here $\Phi \equiv \phi + \omega_0 \tau s$ where $\phi$ is defined as the phase of the complex electrical field $E$. All the ECM solutions $(\Delta, B)$ are fixed points in the phase plane and are located on an ellipse given by $\Delta = \omega_0 \tau + \alpha N \pm \sqrt{\eta^2 - N^2}$. Moreover, the broken lines in the $\Phi(s-1) - \Phi(s)$ vs $s$ diagram correspond to ECM frequencies $\Delta$. (a) $\eta = 4.4$ and the torus has been obtained by progressively increasing $\eta$ from a lower value. (b) $\eta = 4.4$ and the torus has been obtained by progressively decreasing $\eta$ from a larger value.

11
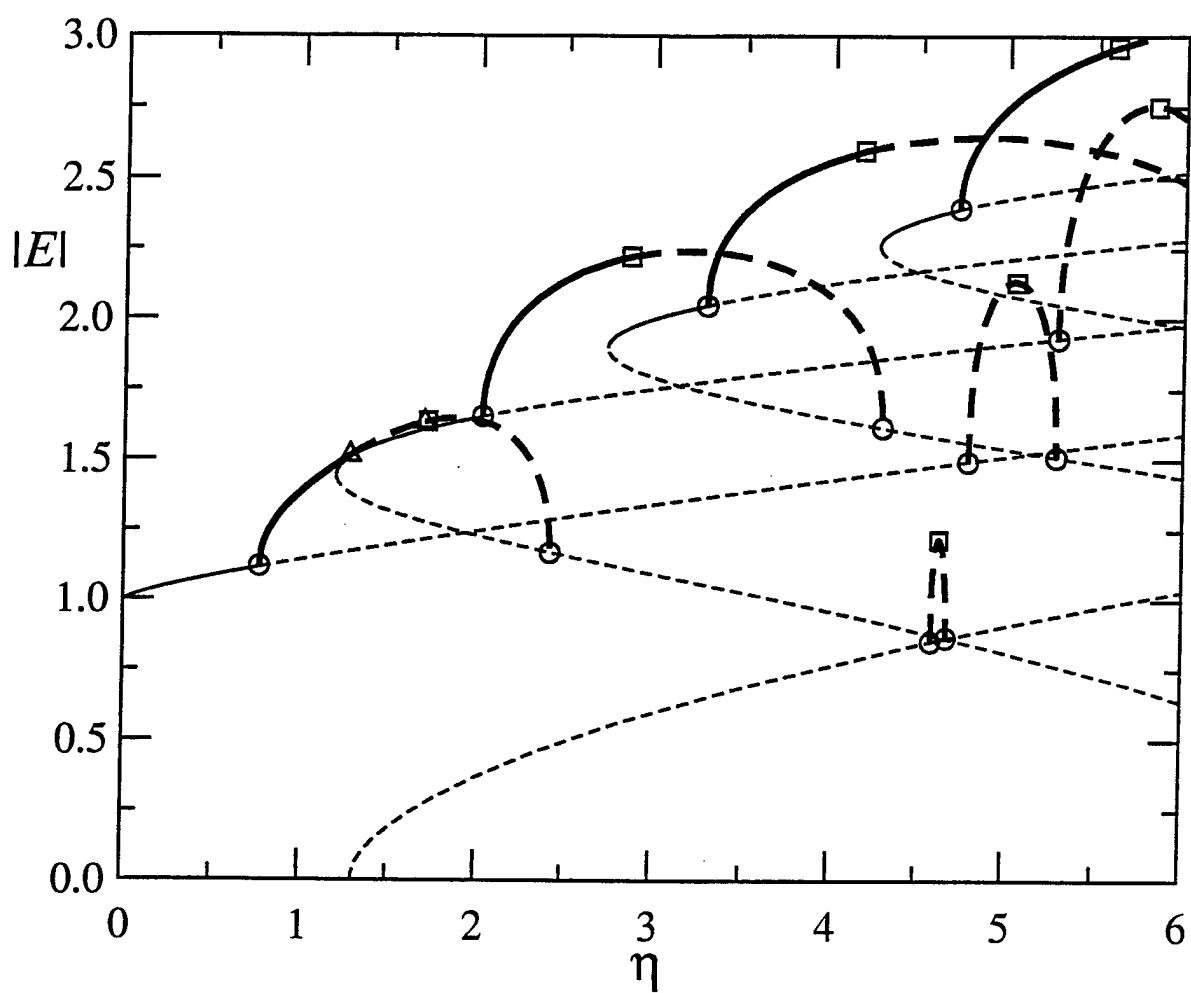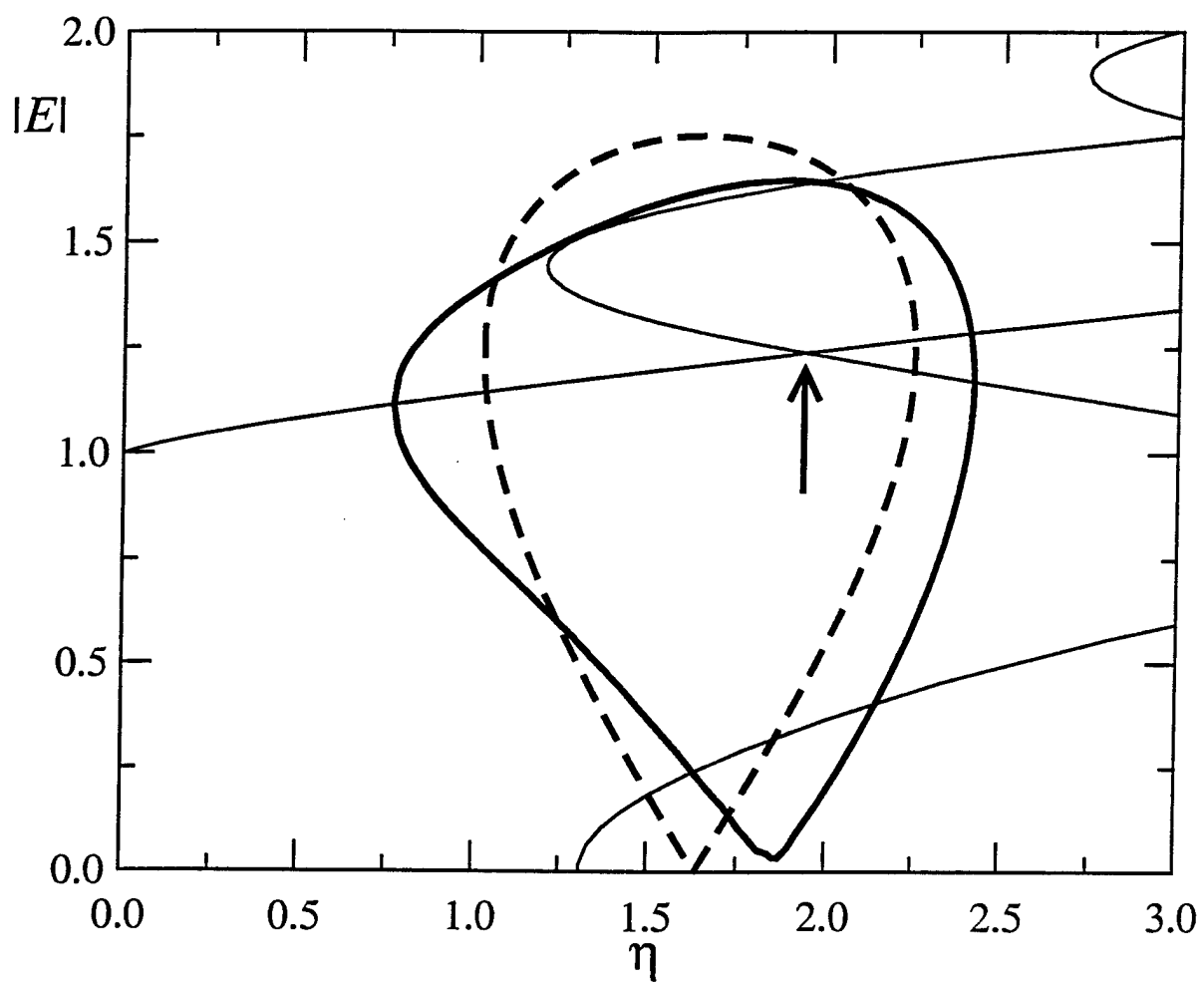
Pieroux et al, Fig 1

Pieroux et al, Fig 2

Pieroux et al. Fig. 3